Finite Element Simulations of Orthogonal Cutting Ti6Al4V Alloy Using Different Cutting Parameters and the Experimental Study

Yicai Shan*

College of Mechanical and Electrical Engineering, Nanjing College of Information Technology, Nanjing, China

*Corresponding author e-mail: shanyc@njcit.cn

Abstract. The finite element simulations of orthogonal cutting Ti6Al4V alloy were carried out based on Abaqus. The Johnson-Cook model was chosen as the constitutive model for the workpiece material, the parameters of the model for Ti6Al4V alloy were obtained through the SHPB (Split Hopkinson Pressure Bar) experiments. The cutting forces and thrust forces got from the simulations using different cutting parameters were observed and validated with the experimental results. A good agreement between the cutting and thrust forces got from the two methods indicated that the parameters of the constitutive model for the Ti6Al4V alloy, which were obtained from the SHPB experiments are correct and the finite element simulations of cutting processes in this work are reliable, so conclusions can be got as: the finite element simulations of metal cutting process can be widely used in practice to study more about the machining process and provide reliable dates for improving the manufacturing efficiency and the property of the machined workpiece in mechanical manufacturing industries.

1. Introduction

In the 21st century, metal cutting will still be a widely used method in mechanical manufacturing field [1-2], furthermore, as there will be more and more precision parts are in great market demand, much higher level demands in metal cutting process will be needed. As the process of metal cutting is so complex that it is almost impossible to study certain characteristics during the cutting process through pure experiments, nowadays, as the fast development of the computer science, it become possible to study the metal cutting process using the finite element simulations, which can help the researches understand more about the mechanism in the metal cutting process and optimize the cutting parameters to reduce the experimental expenses effectively and improve the machined parts' properties to make sure that they can meet the industrial requirements, so it can be said that the role of the finite element simulation of metal cutting in high standard metal cutting is significantly important.

The process of the metal cutting simulations is also complex. The accuracies and the properties of the machined parts will be affected by cutting parameters, geometric parameters of cutting tool and cutting path [3-4], which makes the simulation process difficult.

Titanium alloy Ti6Al4V has received particular consideration since it is a popular material in the aerospace and medical device industries, furthermore, this material produces saw chips under certain cutting conditions, which makes it more remarkable in terms of metal cutting study [5-7].

As to the finite element simulations of Ti6Al4V alloy cutting process, lots of work have been carried out during the past several years [8], in order to make sure the simulation results convincible enough, both the experiments for obtaining the constitutive model parameters for the workpiece material and the simulations of the cutting process were carried out in this work. Using the SHPB experiment, the parameters of the Johnson-Cook constitutive model for Ti6Al4V alloy were obtained, and the correctness of the simulation results was validated by the corresponding experiments at last.

2. Model parameters for workpiece and tool

2.1. Constitutive model for Ti6Al4V alloy

In the machining process, large plastic deformations which are accompanied with high strain rate and high temperature will occur, and the time needed for the chip formation is extremely short, furthermore, the gradients of the temperature, stain and strain rate and in the cutting zone is very high, so a constitutive model considering all the temperature, stain and strain rate effects should be imposed in metal cutting simulations. In the past several years, several constitutive models were proposed by the researchers such as Zerrilli-Armstrong model, Follansbee-Kocks model, Johnson-Cook model, Bodner-Paton model, et al. In the finite element simulations of metal cutting, Johnson-Cook model is the mostly used one [9], and the expression of which can be written as:

$$\sigma = \left[A + B\varepsilon^{n} \right] \left[1 + c \ln \left(\frac{\dot{\varepsilon}}{\dot{\varepsilon}_0} \right) \right] \left[1 - \left(\frac{T - T_r}{T_m - T_r} \right)^{m} \right] \tag{1}$$

In the expression, $\left[A + B\varepsilon^{n} \right]$ considers the effect of strain hardening, $\left[1 + c \ln \left(\frac{\dot{\varepsilon}}{\dot{\varepsilon}_0} \right) \right]$ considers the effect of strain rate hardening, and $\left[1 - \left(\frac{T - T_r}{T_m - T_r} \right)^{m} \right]$ considers the effect of heat softening. T_r is the reference temperature, $\dot{\varepsilon}_0$ is the reference strain rate, the parameters of A, B, n, c, m, D, k need to be obtained from the experiments, the parameters of A, B, n are strain hardening effect dependent, c is strain rate hardening effect dependent, and m is heat softening effect dependent, θ_{m} is the melting point and θ_{t} is the ambient temperature.

In the past several years, the SHPB experiments have been widely adopted for obtaining the Johnson-Cook model parameters for metal materials [10]. In this work, the Johnson-Cook model parameters for Ti6Al4V alloy were also obtained using SHPB experiments under different temperatures and different strain rates. At last, the parameters obtained from the experiments are as shown in Table.1.

Table 1. The parameters of Johnson-Cook plastic model for Ti6Al4V alloy.

Material	A(Mpa)	B(Mpa)	c	n	m
Ti6Al4V	875	793	0.011	0.386	0.71

2.2. Failure criteria for Ti4Al4V alloy

Shear failure model was used to define the failure criteria for Ti4Al4V alloy in this work, which is based on the equivalent plastic strains on integral point. If the value of the failure parameter researches

1, then the material in the cutting zone will be considered to be removed from the workpiece and the corresponding chip will be formed [11]. The expression for the failure parameter can be written as:

$$\omega = \frac{\bar{\varepsilon}_0^{pl} + \Sigma \Delta \bar{\varepsilon}^{pl}}{\bar{\varepsilon}_f^{pl}} \tag{2}$$

Where ω is the failure parameter, $\bar{\varepsilon}_0^{pl}$ is the initial value of the equivalent plastic strain, $\bar{\varepsilon}_f^{pl}$ is the failure strain, $\Delta\bar{\varepsilon}^{pl}$ is the increment of the equivalent plastic strain. The failure parameter, $\bar{\varepsilon}_0^{pl}$ is stain, plastic strain rate and temperature dependent. The Johnson-Cook failure expression can be written as [12]:

$$\bar{\varepsilon}_f^{pl} = \left[d_1 + d_2 \exp\left(d_3 \frac{p}{q}\right)\right]\left[1 + d_4 \ln\left(\frac{\dot{\bar{\varepsilon}}^{pl}}{\dot{\varepsilon}_o}\right)\right]\left(1 + d_5 \hat{\theta}\right) \tag{3}$$

The parameters d_1 - d_5 were got under the transition temperature, $\dot{\varepsilon}_o$ is the reference strain rate, $\dot{\bar{\varepsilon}}^{pl}$ is the plastic strain rate, and the parameter $\hat{\theta}$ can be obtained as:

$$\begin{cases} 0 & for \quad \theta \text{ p } \theta_{transition} \\ (\theta - \theta_{transiton}) / (\theta_{melt} - \theta_{transition}) & for\, \theta_{transition} \le \theta \le \theta_{melt} \\ 1 & for \quad \theta \text{ f } \theta_{melt} \end{cases} \tag{4}$$

Where θ is current temperature, θ_{melt} is the melting point of the workpiece material, $\theta_{transition}$ is the transition temperature. At last, the parameters of d_1 - d_5 were got as -0.09, 0.25, -0.5, 0.0014, 3.87.

2.3. Parameters for tool material

The material of the cutting tool used in the experiment is cemented carbide, which is with density of ρ=15000kg/m3, Young modulus of E=210GP, Poisson's ratio of μ=0.22. And the other parameters for the tool material are as shown in Table 2.

Table 2. The parameters of the cutting tool.

Young modulus(Gpa)	Poisson's ratio	Coefficient of linear expansion (m/m.℃)	Specific heat (J/kg. ℃)	Thermal conductivity (W/m.k)
210	0.22	4.7E-6	200	46

2.4. Friction model

In the process of metal cutting, the frictions between the tool rake face and the newly generated face of the workpiece is very complex. The friction area can be divided into slide area and bonded area. The friction state in the bonded area depends on the critical shear stress of the workpiece material, and the friction force in the slide area can be written as [13-14]:

$$\tau_c = \min(\mu\sigma_n, \tau_s) \tag{5}$$

Where τ_c is the slide friction stress on the rake face, μ is the friction coefficient, σ_n is the normal pressure on the contact area, τ_s is the critical yield stress of the workpiece material. The friction coefficient μ was defined as 0.4 in the modeling here.

2.5. Mesh generation

After the model has been seeded, Quard was chosen as the shape of the mesh. As the temperature effect was considered in the simulations, so Temperature-Displacement coupling was chosen for the element type, also plan stain, secondary accuracy and distortion control were selected, and length ratio was set as 0.8, as for hourglass control, relax stiffness was selected.

3. Finite element modeling

The finite element simulations in this work were based on the assumptions as: (1) there were no vibrations of the cutting tool and the workpiece, (2) the cutting depth always stayed the same, (3) there was no phase transformation or other chemical change in the cutting process caused by the high temperature, (4) the material of the workpiece was isotropic, (5) there was no tool wear in the whole cutting process.

As the strains, stresses and the temperatures in the cutting zone need to be observed in more details, and also to make sure the simulation results accuracy enough, much smaller grids were used in the cutting layer. The movement of the workpiece along the horizontal, vertical directions and the movement of the cutting tool along the vertical direction were all constrained, the movement of the cutting tool along the horizontal direction was defined according to the simulated cutting velocity.

The cutting speed was set as 200m/min, and the feed rate was set as 0.035mm/rev at first, the shape of the chip got from the simulation and that from the experiment using the same cutting parameters are as shown in Fig.1. It can be seen that not only the shape of the chip but also the size of the shear localization obtained from the two different ways are in a good agreement, so the parameters of the Johnson-Cook model for the Ti6Al4V obtained from the SHPB experiment can be preliminarily considered as accurate.

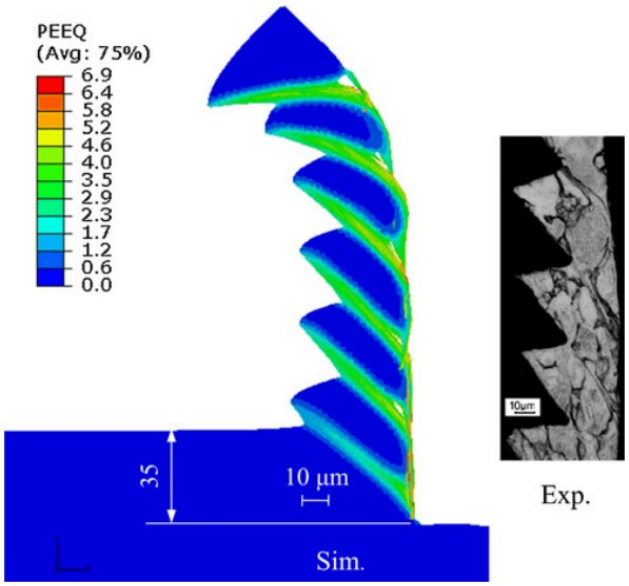

Figure 1. The comparison of the chips obtained from the simulation and that from the experiment.

4. Results and discussion

4.1. The effect of cutting velocity to the results

The cutting forces and thrust forces obtained under different cutting velocities are as shown in Fig.2. In the experiments, the cutting forces were measured using the Kistler9257B three-dimensional dynamometer, The rake angle and radius of the tool nose were all set as 0, the feed rate were all set as 0.2mm/rev,. It can be seen that as the cutting velocity varied from 100m/min to 300m/min, the cutting forces and thrust forces were all increased, although the increment is not obvious. As the cutting speed increased in the above range, the vibration of the cutting force became more gently, so it can be concluded that the machined surface can be improved by higher speed machining. The effect of the cutting velocity to the vibration of the thrust force is not obvious according to the simulations here.

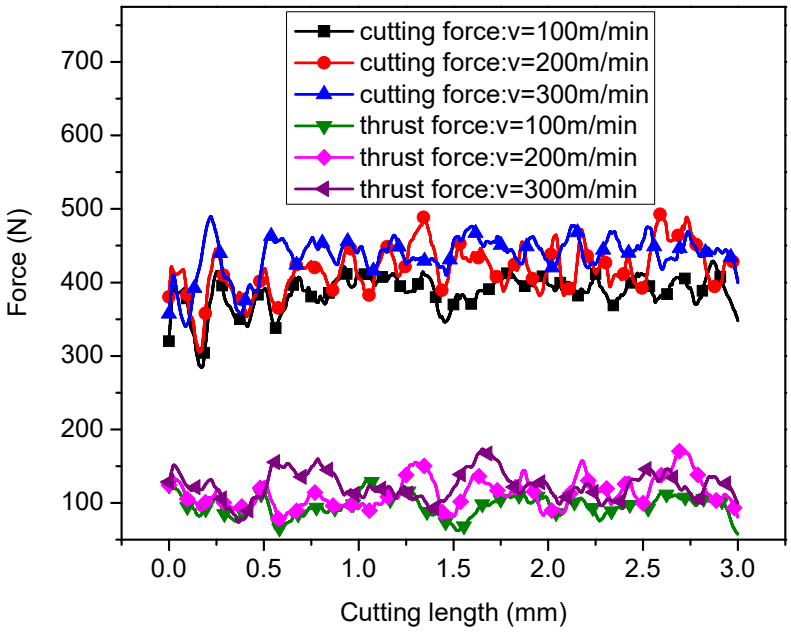

Figure 2. The cutting forces and thrust forces under different cutting velocities.

4.2. The effect of feed rate to the results

The cutting forces and thrust forces obtained under different feed rates are as shown in Fig.3. The rake angle and radius of the tool nose were all set as 0, and the cutting velocity were all set as 300m/min, as the feed rate varied from 0.1mm/rev to 0.3mmrev, it can be seen that the feed rate has a very strong effect on the cutting force, not only the average value of the force, but also the vibration of the force, and the thrust force can also be influenced by the feed rate, although it is not as obvious as the cutting force. According to the simulation results, it can be concluded that as the cutting force vibrated more gently under small feed rate, the machined surface property can be improved with small feed rate.

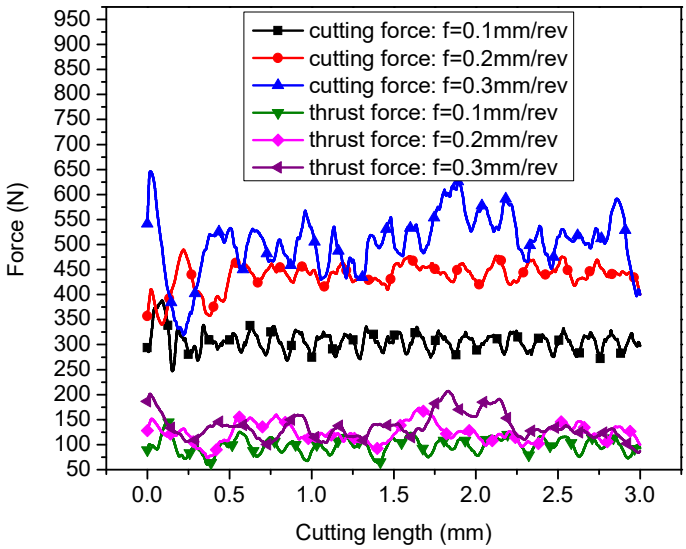

Figure 3. The cutting forces and thrust forces under different feed rates.

4.3. The effect of tool rake angle to the results

The cutting forces and thrust forces obtained under different tool rake angle are as shown in Fig.4. The feed rate was set as 0.2mm/rev, the cutting velocity was set as 300m/min, the tool nose was set as 0. It can be seen that as the rake angle increased from -15° to 15°, the cutting forces and thrust forces all reduced, that may be attributed to that when the rake angle is positive, the cutting angle is sharp, and the cutting force and thrust force of course will be smaller, but when the rale angle is negative, the cutting angle is blunt, so the cutting force and the thrust force will be larger. The effect of the rake angle on the vibration of cutting force is obvious, but its effect on the vibration of the thrust is weak.

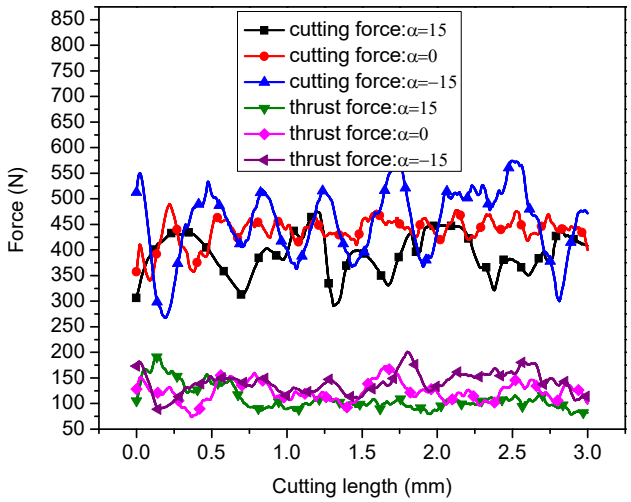

Figure 4. The cutting forces and thrust forces under different tool rake angles.

4.4. The effect of the radius of the tool nose to the results

The cutting forces and thrust forces obtained under different radii of the tool nose are as shown in Fig.5. The cutting velocity were all set as 300m/min, the feed rate were all set as 0.2mm/rev, the rake angle were all set as 0, as the radius of the tool nose varied from 0 to 0.15mm, it can be seen that the cutting force and thrust force all increased as the radius of the tool nose increased in the above range, also the radius of the tool nose also has a strong effect on the vibration of the cutting forces and thrust

forces, as the radius of the tool nose increases, the cutting force and thrust force vibrated more seriously. As to improve the machined surface property, smaller radius of the tool nose should be applied.

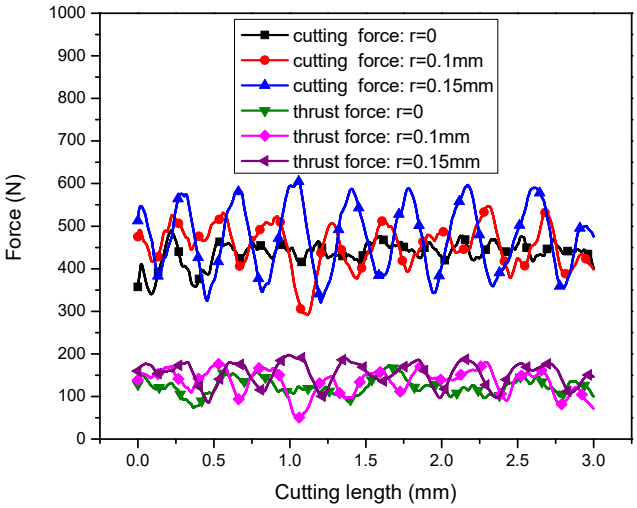

Figure 5. The cutting forces and thrust forces under different radii of the tool nose.

5. Experimental procedures

The corresponding experiments were also carried out to validate the simulation results, the cutting forces, thrust forces and cutting temperatures under different cutting velocities were measured, and a comparison was made between the results got from the two methods.

5.1. The validation of the forces

The comparison between the cutting forces and thrust forces got from the experiments and that from the simulations are as shown in Fig.6. It can be seen that for the cutting forces, the margin of errors are no more than 10% of the maximum force value, as the thrust forces concerned, the margin of errors are no more than 15% of the maximum force value, so it can be concluded that the cutting and thrust forces obtained from the two different methods are in good agreement.

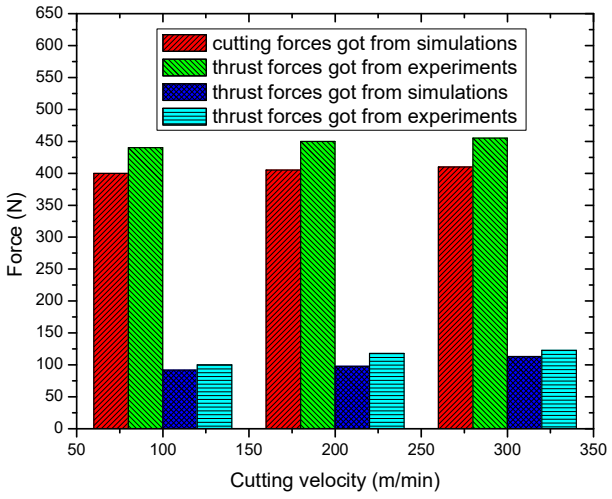

Figure 6. The comparison of the cutting forces and thrust forces obtained from the simulations and that from the experiments.

5.2. The validation of the cutting temperatures

Also the cutting temperatures in the cutting process were measured in the experiments to validate the temperature values got in the simulations. In the experiment, the cutting temperature information was transformed to thermoelectric signals using fast thermocouple calibration device, as shown in Fig.7(b). Considering the effect of the temperature of the cold side of the thermos-electromotive force to the measuring results, the corresponding compensation should be made.

It is almost impossible to get the average temperature value of the cutting zone in the finite element model, as shown in Fig.7(a), so the highest temperatures in the cutting zone was used to compare to the average temperatures obtained from the experiment.

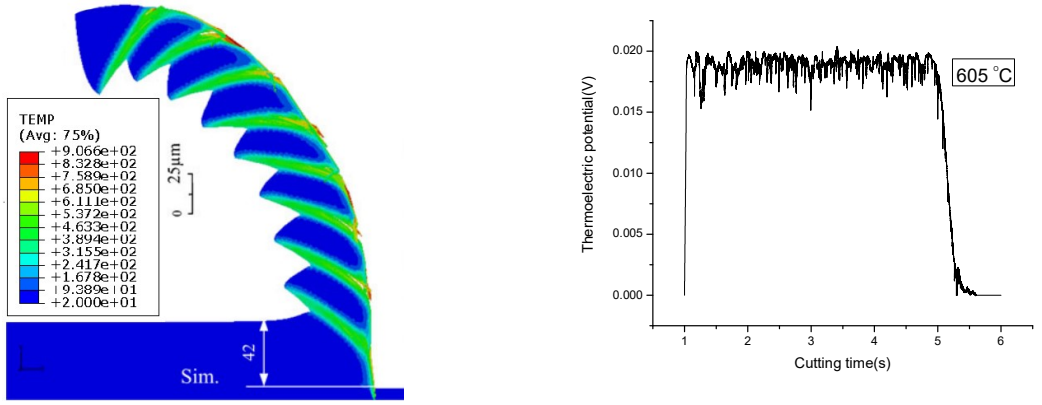

(a) The temperature in the finite element model (b) The thermoelectric signals

Figure 7. The comparison of the cutting temperature in the simulation and that in the experiment at the cutting velocity of 200m/min.

It can be seen that the average temperature obtained from the experiment is about 200℃ lower than the highest temperature in the finite element model, although the difference is obvious, the tendencies of the temperature changing with the cutting velocity are much the same, as shown in Fig.8. Generally speaking, the temperatures got from the simulations are reliable.

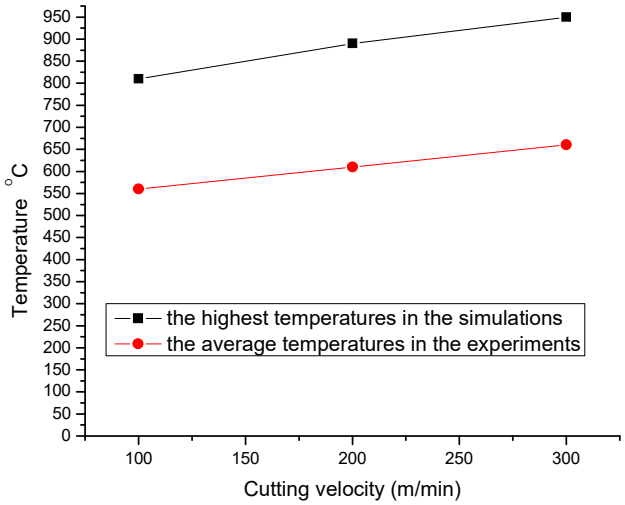

Figure 8. The comparison of the highest temperatures in the simulations and the average temperature in the experiments.

6. Conclusions

Based on the good agreement of the two results obtained from the simulations and that from the experiments, conclusions can be obtained as: the Johnson-Cook constitutive model is suitable to define the relationship between the strains and stresses with considering the effects of strain rates and temperatures in the cutting process, and the constitutive model parameters for titanium alloy Ti6Al4V obtained from the Split Hopkinson Pressure Bar experiments are accurate. According to the simulation results, conclusions can be obtained as: the cutting velocity, feed rate, radius of the tool nose and the tool rake angle, they all have an effect on the cutting force and the thrust force. The effect of the feed rate on the value of the cutting force is very great although its effect on the thrust force is weak, the tool rake angle has a strong effect on the vibration of the cutting forces which may affect the property of the machined surface. According the simulations results obtained from different cutting parameters, in order to improve the machined surface property, high cutting velocity, and small feed rate, positive rake angle and small radius of the tool nose should be used. As proven by the work in this paper, finite element simulation of the metal cutting process can help researchers learn more about the mechanism in the metal cutting process, and optimize the cutting parameters to improve manufacturing efficient and the machined parts' properties. Generally speaking, finite element simulation of the metal cutting process plays a very important role in the manufacturing field.

Acknowledgments

This work has been performed by Innovation Project of Jiangsu Province (2016-12), Jiangsu University of natural science research project (17KJB460008).

References

[1] G. Byrne, D. Dornfeld, B. Denkena, "Advancing cutting technology", CIRP Annals-Manufacturing Technology, vol. 52, no. 2. pp. 483-507, 2003.

[2] L. H. Meng, N. He, Y. F. Yang, W. Zhao, and B. Rong, "Method for Measuring Residual Stresses Induced by Boring in Internal Surface of Tube and Its Validation with XRD Method", Transactions of Nanjing University of Aeronautics and Astronautics, vol. 31, no. 5. pp. 508-514, 2014.

[3] L. H. Meng, N. He, L. Li, Y. F. Yang, and W. Zhao, "Measurement of the Residual Stress Induced by Milling in TC4 Workpiece before Self-Balancing and Its FEA", Rare Metal Materials and Engineering, vol. 43, no. 8. pp. 1991-1996, 2014. (in Chinese)

[4] L. H. Meng, N. He, L. Li, Y. F. Yang, and W. Zhao, "Measurement of Pre-Self-Balanced Surface Residual Stresses Induced by Milling in Titanium Alloys and the FEM Validation", Advanced Materials Research, no. 996. pp. 615-621, 2014.

[5] Y. Karpat, "Temperature dependent flow softening of titanium alloy Ti6Al4V: An investigation using finite element simulation of machining", Journal of Materials Processing Technology, vol.211, no. 4. pp. 737-749, 2011.

[6] L. H. Meng, N. He, L. Li, "Calculation of Residual Stress Induced by Machining in Internal Surface of TC4 Tubular Parts and Its FEA", China Mechanical Engineering, vol. 25, no. 19. pp. 2583-2587, 2014. (in Chinese)

[7] L. H. Meng, N. He, Y. F. Yang, W. Zhao, "Application of FEM correction to measuring the surface residual stresses generated by turning Ti6A14V tube parts", Journal of Harbin Institute of Technology, vol. 47, no. 5. pp. 71-75, 2015. (in Chinese)

[8] Y. C. Yen, P. Sartkulvanich, T. Altan, "Finite element modeling of roller burnishing process", CIRP Annals-Manufacturing Technology, vol. 54, no. 1. pp. 237-240, 2005.

[9] Y. J. Chao, X. Qi, "Thermal and thermo-mechanical modeling of friction stir welding of aluminum alloy 6061-T6", Journal of materials processing and manufacturing science, no. 7. pp. 215-233, 1998.

[10] A. R. Yildiz, "Optimization of cutting parameters in multi-pass turning using artificial bee colony-based approach", Information Sciences, vol. 220. pp. 399-407, 2013.

[11] J. S. Strenkowski, J. T. Carroll, "A finite element model of orthogonal metal cutting", Journal of Manufacturing Science and Engineering, vol. 107, no. 4. pp. 349-354, 1985.
[12] P. V. Bayly, J. E. Halley, B. P. Mann and M. A, "Davies, Stability of interrupted cutting by temporal finite element analysis", Journal of Manufacturing Science and Engineering, vol. 125, no. 2. pp. 220-225, 2003.
[13] H. Bil, S. Kılıç, A. E. Tekkaya, "A comparison of orthogonal cutting data from experiments with three different finite element models", International Journal of Machine Tools and Manufacture, vol. 44, no. 9. pp. 933-944, 2004.
[14] C. Shet, X. Deng, "Finite element analysis of the orthogonal metal cutting process", Journal of Materials Processing Technology, vol. 105, no. 1. pp. 95-109, 2000.